Original Article

Alterations in local activity and whole-brain functional connectivity in human immunodeficiency virus-associated neurocognitive disorders: a resting-state functional magnetic resonance imaging study

Xingyuan Jiang[1], Chuanke Hou[1], Juming Ma[1], Hongjun Li[1,2,3]

[1]Department of Radiology, Beijing Youan Hospital, Capital Medical University, Beijing, China; [2]Beijing Advanced Innovation Centre for Biomedical Engineering, Beihang University, Beijing, China; [3]Laboratory for Clinical Medicine, Capital Medical University, Beijing, China

Contributions: (I) Conception and design: X Jiang, H Li; (II) Administrative support: H Li; (III) Provision of study materials or patients: X Jiang, C Hou, J Ma; (IV) Collection and assembly of data: X Jiang, C Hou, J Ma; (V) Data analysis and interpretation: X Jiang; (VI) Manuscript writing: All authors; (VII) Final approval of manuscript: All authors.

Correspondence to: Hongjun Li, MD. Department of Radiology, Beijing Youan Hospital, Capital Medical University, No. 8, Xitoutiao, You'anmenwai, Fengtai District, Beijing 100069, China; Beijing Advanced Innovation Centre for Biomedical Engineering, Beihang University, No. 85, Hong'an Road, Doudian Town, Fangshan District, Beijing 102433, China; Laboratory for Clinical Medicine, Capital Medical University, No. 10, Xitoutiao, You'anmenwai, Fengtai District, Beijing 100069, China. Email: lihongjun00113@ccmu.edu.cn.

Background: Approximately half of human immunodeficiency virus (HIV) patients experience HIV-associated neurocognitive disorders (HAND); however, the neurophysiological mechanisms underlying HAND remain unclear. This study aimed to evaluate changes in functional brain activity patterns during the early stages of HIV infection by comparing local and global indicators using resting-state functional magnetic resonance imaging (rs-fMRI).

Methods: A total of 165 people living with HIV (PLWH) but without neurocognitive disorders (PWND), 173 patients with asymptomatic neurocognitive impairment (ANI), and 100 matched healthy controls (HCs) were included in the study. A cross-sectional study of the participants was conducted. The metrics of functional segregation and integration were computed, using graph theory to explore differences across methodologies. Brain functional changes in the PWND and ANI groups were assessed, and correlations between the rs-fMRI metrics, clinical data, and cognitive function were examined.

Results: As cognitive function declined, changes reflected by regional homogeneity (ReHo) were primarily observed in the default mode network (DMN). In the DMN and visual network (VIS), amplitude of low-frequency fluctuation (ALFF) decreases were mainly observed in the parieto-occipital lobes, while increases were mainly observed in the limbic network (LIM). Reductions in fractional ALFF (fALFF) were mainly observed in the somatomotor network (SMN) and LIM, while increases were observed in the DMN and LIM. Unlike local indicators, global functional connectivity (FC) significantly decreased in both the PWND and ANI groups compared to the HC group. The ANI group showed partial increases in FC compared to the PWND group, with major changes observed in the DMN, VIS, and LIM. Notably, FC between the right insula and right supramarginal gyrus decreased significantly following HIV infection, while FC between the right caudate nucleus and the left middle frontal gyrus declined further in the ANI group. Graph theory further confirmed the significance of the DMN, and revealed changes in the eigenvector centrality mapping (ECM) values of the frontoparietal network (FPN) and dorsal attention network (DAN).

Conclusions: HIV patients exhibit complex changes in both local and global brain activity, regardless of cognitive impairment. Widespread abnormalities primarily involve the DMN, VIS, and LIM. Changes in FC along the fronto-striatal pathway may play a crucial role in the decline of cognitive function in individuals

with HAND. Our findings provide new insights that may assist in the early detection of brain damage in the early stages of HIV infection. The use of multiple methodologies may offer a more comprehensive and effective approach, enabling the early detection of brain damage in HIV patients.

Keywords: Human immunodeficiency virus-associated neurocognitive disorders (HAND); resting-state functional magnetic resonance imaging (rs-fMRI); regional homogeneity (ReHo); amplitude of low-frequency fluctuation (ALFF); functional connectivity (FC)

Submitted Jul 02, 2024. Accepted for publication Nov 06, 2024. Published online Dec 11, 2024.
doi: 10.21037/qims-24-1342
View this article at: https://dx.doi.org/10.21037/qims-24-1342

Introduction

With the widespread use of combination antiretroviral treatment (cART), acquired immunodeficiency syndrome (AIDS) has transformed into a chronic disease. However, approximately half of people living with human immunodeficiency virus (PLWH) gradually experience cognitive and motor function decline, leading to the development of human immunodeficiency virus-associated neurocognitive disorders (HAND) (1,2). Asymptomatic neurocognitive impairment (ANI) represents both the early stage and most common form of HAND, making it a crucial reversible period for HAND prevention and intervention (3,4). Regular screening with HAND scales serves as a valuable tool for the early diagnosis, monitoring of neurocognitive function, and assessment of treatment efficacy. However, these scales have several limitations in clinical application, such as being time consuming, and having low thresholds and high subjectivity. Moreover, they cannot be used to evaluate the extent of brain damage in PLWH. Therefore, non-invasive and precise detection methods for early brain damage in PLWH using magnetic resonance imaging (MRI) need to be established to explore the patterns and mechanisms of HAND development and evolution, and to identify alternative indicators.

In 1995, it was first demonstrated that correlations exist between activated brain regions at rest and in task states (5), and that resting-state functional magnetic resonance imaging (rs-fMRI) can capture brain trends that task-based functional magnetic resonance imaging (fMRI) cannot (6). Consequently, rs-fMRI has gained prominence as an alternative to task-based fMRI. Rs-fMRI measures spontaneous blood-oxygen-level-dependent (BOLD) signal activity, with fluctuations in signal amplitude typically occurring in the 0.01 to 0.1 Hz range (7). In rs-fMRI, the brain is considered a unified network, and functional segregation metrics focus on the localized activity of certain brain areas, while functional integration metrics highlight the interactions or connectivity between various brain regions (8).

Both regional homogeneity (ReHo) and amplitude of low-frequency fluctuation (ALFF) reflect neural activity at the regional level, and are commonly used to evaluate functional segregation. ReHo measures the consistency and centrality of regional activity by analyzing specific voxels and their relationships with adjacent voxels, testing their activity correlations through Kendall's coefficient of concordance (KCC) (9). Conversely, ALFF focuses on the intensity of spontaneous brain activity within local regions, measuring the total power of BOLD signals in the low-frequency range of 0.01 to 0.1 Hz (10). One limitation of ALFF is its sensitivity to background noise and voxels near large vascular structures, which led to the introduction of fractional ALFF (fALFF). fALFF represents the proportion of the ALFF signal in each voxel relative to the total power of signals over the full frequency spectrum, thus enhancing both sensitivity and specificity in detecting spontaneous brain activity (11).

Multiple studies have reported alterations in local functional metrics in the brains of human immunodeficiency virus (HIV) patients, including regions such as the striatum, frontal lobe, occipital lobe, and temporal lobe. These functional metrics may be related to neurocognitive functions, such as learning, memory, and executive function (12-15). Functional integration examines the interactions between different brain regions or networks by assessing functional connectivity (FC), revealing more global trends (16). Research on FC between multiple regions has also revealed significant changes in interactions among different brain regions in HIV patients, with studies reporting both increases and decreases in FC, and some

even presenting inconsistent results (17,18). Additionally, some studies have reported that HIV selectively disrupts brain regions, such as the default mode network (DMN) and frontoparietal network (FPN), alters FC between regions, may be associated with declines in executive function, and may accelerate brain aging (19,20).

ReHO, ALFF, and fALFF are potential methods for investigating global FC. However, the most common and reliable approach for quantifying local connectivity involves graph theory metrics, such as eigenvector centrality (EC), global efficiency, and local efficiency (21). Node efficiency (NE) quantifies a network's capacity for parallel information transmission, with higher NE values indicating stronger multithreaded processing capabilities. Local node efficiency (NLE) measures a network's resilience to small-scale failures (fault tolerance) and its compensatory ability, with higher NLE values signifying greater stability. Eigenvector centrality mapping (ECM) spatially characterizes FC in functional brain imaging by attributing network characteristics to individual voxels. The ECM method is based on the concept of EC, which represents functionally active networks over time, and assigns centrality values to each region of interest (ROI) based on the centrality properties of directly neighboring ROIs in the functional network (22). Although previous studies have explored graph theory in the context of HIV, none have conducted comparative analyses of these methods (23). Therefore, it was thought that combining local and global metrics might provide comprehensive imaging biomarkers for early brain functional changes in HAND.

To avoid the impact of aging on brain function, this study focused on young Chinese men who have sex with other men. The following three groups were included in the study: the ANI group; the PLWH but without neurocognitive disorders (PWND) group; and the healthy control (HC) group. We extracted and analyzed ReHo, ALFF, fALFF, and FC metrics from rs-fMRI. Further, we employed graph theory methods to assess the NE, NLE, and ECM metrics. We sought to identify neuroimaging characteristics of brain function in ANI patients and to explore correlations between neuroimaging metrics, cognitive function, and clinical information. Our findings provide critical scientific evidence for the early diagnosis, identification of intervention targets, and adjunctive treatment of ANI patients, and offer valuable insights into the neuropathophysiological mechanisms of the ANI stage. We present this article in accordance with the STROBE reporting checklist (available at https://qims.amegroups.com/article/view/10.21037/qims-24-1342/rc).

Methods

Participants

This study was conducted in accordance with the Declaration of Helsinki (as revised in 2013) and was approved by the Medical Ethics Committee of Beijing Youan Hospital (No. LL-2020-047-K). All the participants were recruited from the Beijing Youan Hospital and provided written informed consent. Given that over 90% of the HIV-positive participants in this study were right-handed males, and previous research has reported significant correlations between hand dominance, gender, brain structure, and function (24), the study population comprised right-handed Chinese HIV-infected males aged 20–50 years. HIV infection was confirmed via immunoblotting or polymerase chain reaction. Patients were excluded from the study if they met any of the following exclusion criteria: (I) had neurological diseases causing cognitive impairment such as brain tumors, infections, stroke, or epilepsy; (II) had psychiatric disorders, including depression and anxiety; (III) had a history of substance abuse, alcohol abuse, or drug addiction; (IV) had claustrophobia or MRI contraindications such as pacemakers, mechanical heart valves, or defibrillators; and/or (V) had severe visual, hearing, or reading difficulties (25). A total of 397 HIV-infected participants were recruited from the Sexually Transmitted Disease and AIDS Clinic of Youan Hospital, and 123 HIV-negative HCs were recruited from the community.

Neuropsychological assessment

The Activity of Daily Living scale and Hamilton Depression Rating Scale (HAMD) (26) were used to assess daily functioning, and exclude participants with significant depression (as indicated by a HAMD score <7). A detailed neuropsychological assessment was conducted using validated Chinese versions of cognitive assessments adjusted for age, education, and place of residence (27), covering the six cognitive domains listed in *Table 1*. Raw scores from the nine subtests were transformed into normative t scores for the six cognitive domains. The ANI diagnosis was based on the Frascati criteria: (I) a performance below 1 standard deviation in ≥2 cognitive domains adjusted for demographics; (II) no decline in daily functioning; (III)

Table 1 Cognitive domains and corresponding neurocognitive scales

Cognitive domains	Neurocognitive scales
Verbal and language	Animal verbal fluency test (AFT)
Attention/working memory	(I) Continuous performance test-identical pair (CPT-IP)
	(II) Wechsler memory scale (WMS-III)
	(III) Paced auditory serial addition test (PASAT)
Memory (learning and recall)	(I) Hopkins verbal learning test (HVLT-R)
	(II) Brief visuospatial memory test (BVMT-R)
Abstraction/executive	Wisconsin card sorting tests (WCST-64)
Speed of information processing	Trail marking test A (TMT-A)
Fine motor skills	Grooved pegboard

Table 2 Demographic, clinical variables, and neuropsychological data

Variables	PWND (n=165)	ANI (n=173)	HCs (n=100)	P value
Age (years)	34.0 (29.0–38.0)	33.0 (30.0–38.0)	32.0 (28.0–36.5)	0.077[a]
Education level (years)	16.0 (15.0–16.0)	15.0 (15.0–16.0)	16.0 (12.0–18)	0.110[a]
Disease course (months)	57.5 (31.0–86.0)	52.5 (29.0–74.0)	–	0.131[b]
Plasma VL (HIV RNA load)	TND	TND	–	–
$CD4^+$ (cells/μL)	600.0 (425.5–796.0)	549.0 (392.0–740.0)	–	0.145[b]
$CD4^+/CD8^+$ ratio	0.7 (0.5–0.9)	0.6 (0.4–0.9)	–	0.456[b]
Scores of cognitive performance				
Verbal and language	51.8±9.3	48.2±9.3	–	<0.001[c]
Attention/working memory	44.0 (40.2–49.5)	37.2 (32.5–42.2)	–	<0.001[b]
Memory (learning and recall)	47.0 (42.0–53.0)	41.0 (34.0–48.0)	–	<0.001[b]
Abstraction/executive	47.0 (42.5–51.5)	37.0 (32.0–42.0)	–	<0.001[b]
Speed of information processing	46.0±8.2	41.3±9.7	–	<0.001[c]
Fine motor stills	47.0 (42.0–51.0)	44.0 (39.0–51.0)	–	<0.001[b]

Data are presented as median (IQR) or mean ± SD. [a], the Kruskal-Wallis test; [b], the Wilcoxon rank-sum test; and [c], the *T*-test. Infection duration (months), current CD4 count, CD4/CD8 ratio, attention and working memory, memory (learning and recall), abstraction and executive function, and fine motor skills are described using medians and IQRs, and were compared using the Wilcoxon rank-sum test. Age and education level are described using medians and IQRs, and were compared using the Kruskal-Wallis test. Verbal and language skills and information processing speed are described using means and standard deviations, and were compared between groups using the *T*-test. PWND, people living with human immunodeficiency virus but without neurocognitive disorders; ANI, asymptomatic neurocognitive impairment; HCs, healthy controls; VL, viral load; HIV, human immunodeficiency virus; TND, target not detected; IQR, interquartile range; SD, standard deviation.

impairments that do not meet the delirium or dementia criteria; (IV) no alternative cause for ANI (3). Of the 397 participants, 193 were diagnosed with PWND and 204 with ANI, with cognitive differences detailed in *Table 2*.

Imaging acquisition and processing

All images were acquired using a 3.0 T MRI scanner with a 32-channel head coil (Siemens Trio Tim, Erlangen, Germany). During the rs-fMRI data acquisition, the

participants were instructed to keep their eyes closed, remain awake, and relax. T1-weighted structural images were acquired using the following magnetization-prepared rapid gradient-echo sequence: repetition time (TR) =1,900 ms, echo time (TE) =2.52 ms, inversion time (TI) =900 ms, acquisition matrix =256×246, field of view =250 mm × 250 mm, flip angle =9°, and voxel resolution =1 mm × 1 mm × 1 mm. Functional imaging was conducted using the following gradient-echo single-shot echo planar imaging (EPI) sequence: TR =2,000 ms, TE =30 ms, acquisition matrix =64×64, voxel size =3.5 mm × 3.5 mm, and flip angle =90°. A total of 240 time points (35 slices) were acquired over an 8-minute period. Data preprocessing was performed using the Statistical Parametric Mapping 12 (SPM12) software package (http://www.fil.ion.ucl.ac.uk/spm/software/spm12/) and the GRETNA toolbox (https://www.nitrc.org/projects/gretna/). Functional images were first converted to the neuroimaging informatics technology initiative (NIFTI) format. The first 10 images were discarded to account for magnet stabilization, after which, slice timing correction and realignment for head motion correction were performed, and participants with translations >3.5 mm or rotations >3.5° were excluded. Spatial normalization was performed using T1 segmentation, and linear trends were removed. The Friston-24 head motion parameters, along with white matter and cerebrospinal fluid signals, were included as covariates and regressed out, and temporal band-pass filtering was then performed (0.01–0.1 Hz).

ReHo brain maps were constructed using DPARSF software (http://www.restfmri.net/) by computing the KCC of the time series of each voxel with its 26 neighboring voxels (28). Each voxel's ReHo value was then normalized and smoothed with an 8 mm Gaussian kernel to reduce noise and enhance statistical efficiency.

ALFF was calculated using DPARSF software. For a given voxel, the filtered time series was transformed to the frequency domain via fast Fourier transform to obtain the power spectrum, and the square root of the power spectrum was then taken and averaged in the 0.01–0.1 Hz range (11). Z-standardized ALFF maps were generated for each participant.

FC networks were constructed using GRETNA. The whole brain was parcellated into 90 ROIs from the automated anatomical labeling template. Network edges were defined by extracting mean time series for each ROI and computing Pearson correlations between each pair of ROIs (29). Fisher's Z transformation was applied to the correlation matrices.

Due to motion and registration issues, the imaging results of 28 PWND, 31 ANI, and 23 HC participants were excluded.

Graph theoretical analysis

GRETNA 2.0 software was employed to compute the area under the curve (AUC) for the topological characteristics of nodes throughout the entire brain network across various threshold ranges. These AUC values were then used for the statistical analyses. The NE was defined as the inverse of the average total of the shortest path lengths from a specific node to all other nodes, while the NLE was defined as the efficiency of information communication among a node's neighbors when that node was excluded.

In our study, we employed the fast fECM toolbox to estimate voxel-wise EC from the time-series data defined by the Harvard-Oxford ROIs for each participant (30). The ECM was estimated based on an adjacency matrix that contained pairwise correlations between the ROIs. To derive real-valued EC values, we incremented each entry in the adjacency matrix by +1 (31). A specific node could have multiple EC values; however, only the eigenvector corresponding to the highest eigenvalue (EV) was selected for further analysis. At the group level, the highest EVs were averaged across all participants, and only those ROIs with EC coefficients exceeding the 95th percentile (top 5%) were deemed the most central for subsequent analyses. In addition, we evaluated potential variations in influential centers between groups by performing label permutations over 10,000 iterations. ROIs with P values ≤0.05 were considered statistically significant, and the influential centers were classified accordingly. A family-wise error (FWE) correction was implemented for the group-level comparisons but not for the overall count of the ROIs assessed, with only the FWE-corrected P values being reported (32).

Statistical analysis

A statistical analysis of demographic, clinical, and neuropsychological data was performed using IBM SPSS Statistics 29.0 (http://www.fil.ion.ucl.ac.uk/spm/). Continuous variables following a normal distribution are described as the mean ± standard deviation, and were compared using analysis of variance or the *t*-test; non-normally distributed variables are described as the median and interquartile range, and were compared using the

Kruskal-Wallis or Wilcoxon rank-sum test.

Network-based statistics (NBS) were employed to analyze FC. Two-sample *t*-tests were conducted for each group comparison as follows: (I) HCs *vs.* PWND; (II) HCs *vs.* ANI; (III) PWND *vs.* ANI, with age and education as covariates. A primary threshold (P<0.001) was set to detect component size, followed by non-parametric permutation testing (10,000 permutations) to determine statistical significance (corrected P<0.05). GRETNA was used for the network analysis, and the results were visualized using BrainNet Viewer (http://www.nitrc.org/projects/bnv/).

ReHo, ALFF, fALFF, and FC values related to abnormal clusters were obtained and analyzed using DPABI software (http://rfmri.org/DPABI). Relationships between these imaging changes and clinical factors (e.g., neurocognitive test scores and duration of the disease) in patients with ANI were examined by Pearson correlation analyses. Since this study was exploratory in nature, Bonferroni correction was not applied to the correlation results.

Results

Demographic, clinical, and neuropsychological data

A total of 165 patients with PWND, 173 patients with ANI, and 100 HCs were enrolled in this study. The demographic data, clinical characteristics, and neurocognitive test results of all patients and HCs are presented in *Table 2*. There were no significant demographic differences among the three groups. However, the ANI group exhibited significantly lower T scores across all six cognitive domains than the PWND group. This indicates that cognitive dysfunction persists despite viral suppression and immune recovery.

ReHo analysis

Two-sample *t*-tests indicated significant differences in ReHo values across three regions when comparing the PWND and HC groups. Specifically, the left cuneus and right posterior cingulate cortex showed increased ReHo values, while the right orbital middle frontal gyrus exhibited decreased ReHo values in the PWND group compared to the HC group [Gaussian random field (GRF) corrected: P<0.05, with age and years of education as covariates] (*Figure 1* and *Table 3*). Due to GRF correction constraints, P<0.001 was chosen for the HC, ANI, and PWND groups. The results showed increased ReHo values in the bilateral posterior cingulate cortex in the ANI group relative to the HC group, and decreased ReHo values in the left parahippocampal gyrus in the ANI group compared to the PWND group; the results are detailed in the Table S1.

ALFF analysis

Two-sample *t*-tests indicated that compared to the HC group, the PWND group had increased ALFF values in the right orbital superior frontal gyrus, and decreased ALFF values in the left angular gyrus. The ANI group had higher ALFF values in the left supplementary motor area and the left triangular portion of the inferior frontal gyrus, but had lower ALFF values in the left middle occipital gyrus. Compared to the PWND group, the ANI group had increased ALFF values in the right insula and right superior temporal gyrus, and decreased ALFF values in the left middle occipital gyrus (GRF corrected: P<0.05, with age and years of education as covariates) (*Figure 1* and *Table 3*).

fALFF analysis

Two-sample *t*-tests revealed that compared to the HC group, the PWND group had increased fALFF values in the right precuneus and decreased fALFF values in the right lentiform nucleus. The ANI group had increased fALFF values in the right thalamus, right paracentral lobule, and right superior temporal gyrus. Compared to the PWND group, the ANI group had increased fALFF values in the left middle temporal gyrus and right insula, and decreased fALFF values in the left rectus gyrus and right paracentral lobule (GRF corrected: P<0.05, with age and years of education as covariates) (*Figure 1* and *Table 3*).

FC

Two-sample *t*-tests showed 233 significant differential connections in the PWND group compared to the HC group, all of which were weakened. The most notable reductions were between the right insula and right supramarginal gyrus (NBS corrected, P<0.05, with age and years of education as covariates). The ANI group exhibited 55 significant differential connections compared to the HC group, all of which were weakened, with the most pronounced decreases between the right caudate nucleus and left middle frontal gyrus (NBS corrected, P<0.05, with

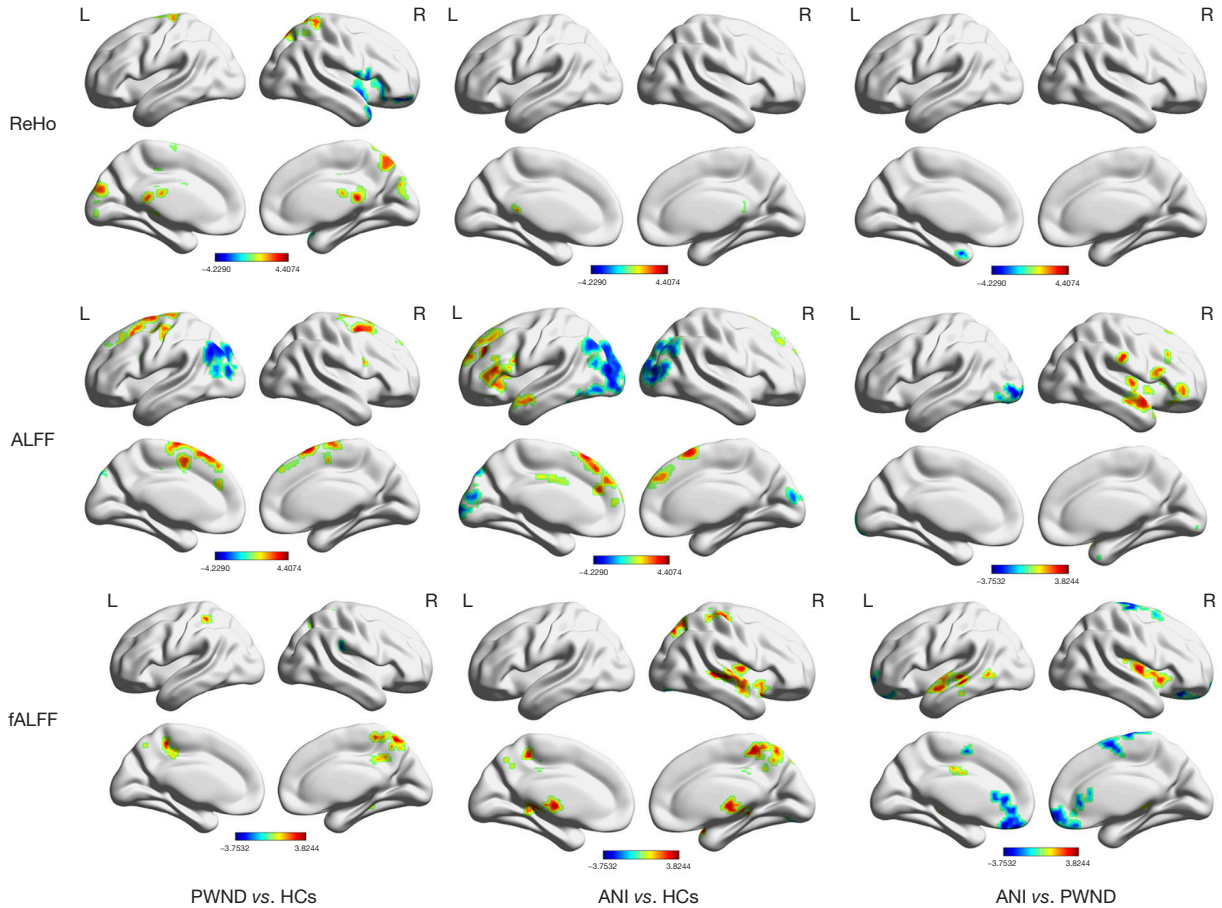

Figure 1 Brain regions with significant differences in rs-fMRI local measures between groups. (Top) Regions with significant differences in ReHo between the two groups. (Middle) Regions showing significantly different ALFF between the two groups. (Bottom) Regions showing significantly different fALFF between the two groups. The color bar represents the range of *T* values. L, left; R, right; PWND, persons living with human immunodeficiency virus but without neurocognitive disorders; ANI, asymptomatic neurocognitive impairment; HCs, healthy controls; rs-fMRI, resting-state functional magnetic resonance imaging; ReHo, regional homogeneity; ALFF, amplitude of low-frequency fluctuation; fALFF, fractional amplitude of low-frequency fluctuation.

age and years of education as covariates). Compared to the PWND group, the ANI group showed 211 significant differential connections, with the most significant reductions between the left opercular part of the inferior frontal gyrus and left superior temporal gyrus, and the most significant increases between the left superior occipital gyrus and right paracentral lobule (P<0.05, with age and years of education as covariates) (*Figure 2*).

NE

The two-sample *t*-test revealed significant intergroup differences in NE values between the PWND and HC groups in three specific regions: compared to the HC group, patients in the PWND group exhibited increased NE values in the left posterior cingulate gyrus and right angular gyrus, while the NE value in the right precentral gyrus was significantly decreased (P<0.05). Similarly, there were significant intergroup differences in the NE values between the ANI and HC groups across three regions: patients in the ANI group had increased NE values in both hippocampi compared to the HC group, while the NE value in the right fusiform gyrus was significantly decreased (P<0.05) (*Figure 3* and *Table 4*). No significant differences in NE values were observed between the ANI and PWND groups in any brain regions.

Table 3 Regions showing significant differences in rs-fMRI values between the groups

Variables	Contrast	Region	Network	MNI coordinates			*T* value	Cluster size
				X	Y	Z		
ReHo	PWND > HCs	Cuneus_L	VIS	–3	–84	24	3.25988	585
		Cingulum_Post_R	DMN	6	–36	15	4.40742	490
	PWND < HCs	Frontal_Mid_Orb_R	FPN	27	45	–15	–4.22899	404
ALFF	PWND > HCs	Frontal_Sup_R	LIM	18	12	54	4.05571	1,660
	PWND < HCs	Angular_L	DMN	–45	–63	33	–3.67434	543
	ANI > HCs	Supp_Motor_Area_L	DAN	–9	24	57	3.67247	833
		Frontal_Inf_Tri_L	FPN	–36	–3	33	3.62824	543
	ANI < HCs	Occipital_Mid_L	VIS	–36	–84	15	–3.68603	1,278
	ANI > PWND	Insula_R	VAN	36	21	15	3.8244	429
		Temporal_Pole_Sup_R	LIM	63	6	–12	3.45091	397
	ANI < PWND	Occipital_Mid_L	VIS	–15	–105	–6	–3.75324	439
fALFF	PWND > HCs	Precuneus_R	DMN	9	–63	57	3.58098	233
	PWND < HCs	Putamen_R	VAN	27	–21	9	–4.2381	270
	ANI > HCs	Thalamus_R	LIM	6	–42	–27	3.97027	406
		Paracentral_Lobule_R	SMN	9	–39	60	3.55937	393
		Temporal_Pole_Sup_R	LIM	39	12	–21	3.47419	338
	ANI > PWND	Temporal_Mid_L	DMN	–60	–24	–6	3.89777	447
		Insula_R	VAN	36	–12	6	3.866	262
	ANI < PWND	Rectus_L	LIM	0	54	–27	–3.95991	545
		Paracentral_Lobule_R	SMN	9	–27	78	–3.76714	273

Coordinates (X, Y, Z) refer to the peak MNI coordinates of brain regions with peak intensity. A positive *t* value indicates increased rs-fMRI values, while a negative *t* value indicates decreased rs-fMRI values. The significance threshold was set at P<0.05. rs-fMRI, resting-state functional magnetic resonance imaging; MNI, Montreal Neurological Institute; ReHo, regional homogeneity; ALFF, amplitude of low-frequency fluctuation; fALFF, fractional amplitude of low-frequency fluctuation; PWND, persons living with human immunodeficiency virus but without neurocognitive disorders; ANI, asymptomatic neurocognitive impairment; HCs, healthy controls; L, left; R, right; VIS, visual network; DMN, default mode network; FPN, frontoparietal network; LIM, limbic network; DAN, dorsal attention network; VAN, ventral attention network; SMN, somatomotor network.

NLE

The two-sample *t*-test revealed significant intergroup differences in NLE values between the PWND and HC groups across five specific regions: compared to the HC group, patients in the PWND group exhibited increased NLE values in the left orbitofrontal gyrus and right parahippocampal gyrus, but exhibited significant decreases in the right medial and paracingulate gyrus, and the bilateral superior temporal gyrus (P<0.05). In comparisons of the ANI and HC groups, significant differences in NLE values were found in three regions: ANI group patients showed increased NLE values in the left hippocampus compared to the HC group, while bilateral insula NLE values were significantly decreased (P<0.05). Further, the ANI and PWND groups displayed significant differences in NLE values across four regions: ANI group patients had increased NLE values in the right medial and paracingulate gyrus, as well as in the left precuneus, compared to the PWND group. Conversely, significant reductions in NLE values were observed in the right dorsolateral superior frontal gyrus and left straight gyrus

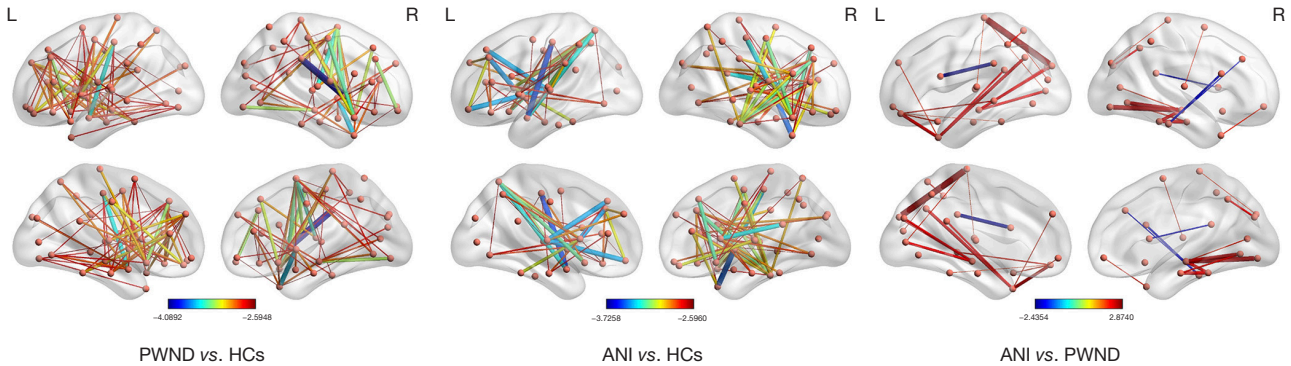

Figure 2 Brain regions with significant differences in FC measures between groups. The left, middle, and right panels respectively show schematic diagrams of brain regions with significant FC differences among the three groups. The lines depict significant FC differences between each pair of specified ROIs, with the color and thickness reflecting the absolute *T*-score value. L, left; R, right; PWND, persons living with human immunodeficiency virus but without neurocognitive disorders; ANI, asymptomatic neurocognitive impairment; HCs, healthy controls; FC, functional connectivity; ROIs, regions of interest.

Table 4 Regions showing significant differences in NE and NLE between the groups

Variables	Contrast	Region	Network	P value	*T* value
NE	PWND > HCs	Cingulum_Post_L	DMN	0.027	2.220
		Angular_R	DMN	0.018	2.380
	PWND < HCs	Precentral_R	DMN	0.023	–2.285
	ANI > HCs	Hippocampus_L	DMN	0.033	2.143
		Hippocampus_R	DMN	0.023	2.285
	ANI < HCs	Temporal_Inf_R	DAN	0.033	–2.137
NLE	PWND > HCs	Frontal_Inf_Orb_L	DMN	0.016	2.419
		ParaHippocampal_R	DMN	0.036	2.112
	PWND < HCs	Cingulum_Mid_R	VAN	0.021	–2.324
		Temporal_Sup_L	SMN	0.018	–2.378
		Temporal_Sup_R	SMN	0.009	–2.628
	ANI > HCs	Hippocampus_L	DMN	0.023	2.286
	ANI < HCs	Insula_L	VAN	0.017	–2.398
		Insula_R	VAN	0.033	–2.142
	ANI > PWND	Cingulum_Post_R	VAN	0.040	2.057
		Precuneus_L	DMN	0.010	2.604
	ANI < PWND	Frontal_Sup_R	DMN	0.046	–2.005
		Rectus_L	LIM	0.041	–2.056

Coordinates (X, Y, Z) refer to the peak MNI coordinates of brain regions with peak intensity. A positive *t* value indicates increased rs-fMRI values, while a negative *t* value indicates decreased rs-fMRI values. The significance threshold was set at P<0.05. NE, node efficiency; NLE, local node efficiency; PWND, persons living with human immunodeficiency virus but without neurocognitive disorders; ANI, asymptomatic neurocognitive impairment; HCs, healthy controls; L, left; R, right; DMN, default mode network; DAN, dorsal attention network; VAN, ventral attention network; SMN, somatomotor network; LIM, limbic network; MNI, Montreal Neurological Institute.

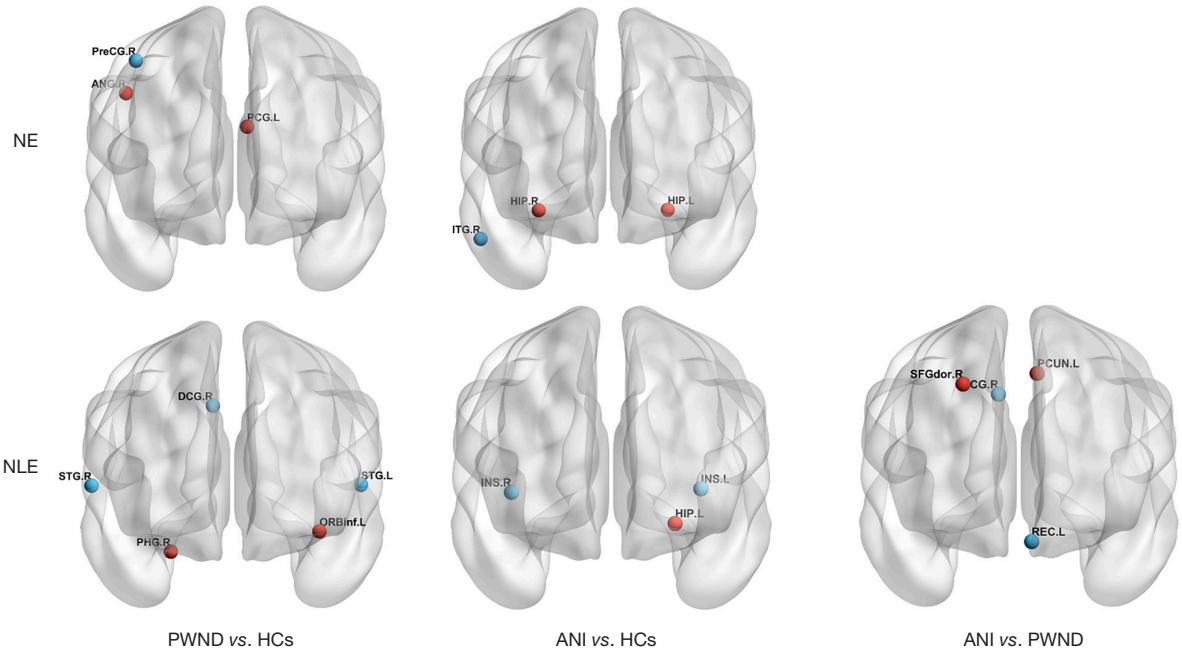

Figure 3 Brain regions with significant differences in NE and NLE metrics between groups. (Top) Regions showing significant differences in NE between the two groups. Red indicates that the NE value in the PWND group is greater than that in the HC group, while blue indicates that the NE value in the PWND group is less than that in the HC group. (Bottom) Regions showing significant differences in NLE between the two groups. Red indicates that the NLE value in the ANI group is greater than that in the PWND group, while blue indicates that the NLE value in the ANI group is less than that in the PWND group. NE, node efficiency; NLE, local node efficiency; PCG.L, left posterior cingulate gyrus; ANG.R, right angular gyrus; PreCG.R, right precentral gyrus; HIP.L, left hippocampus; HIP.R, right hippocampus; ITG. R, right inferior temporal gyrus; DCG.R, right medial and paracingulate gyrus; STG.R, right superior temporal gyrus; STG.L, left superior temporal gyrus; PHG. R, right parahippocampal gyrus; ORBinf.L, left orbitofrontal gyrus; INS.L, left insula; INS.R, right insula; PCUN. L, left precuneus; SFGdor.R, right dorsolateral superior frontal gyrus; REC.L, left straight gyrus; PWND, persons living with human immunodeficiency virus but without neurocognitive disorders; ANI, asymptomatic neurocognitive impairment; HCs, healthy controls.

(P<0.05) (*Figure 3* and *Table 4*).

ECM

The two-sample *t*-test revealed significant intergroup differences in the ECM values between the PWND and HC groups in two specific regions: compared to the HC group, patients in the PWND group exhibited increased ECM values in the left medial and paracingulate gyrus, while the ECM value in the right precentral gyrus decreased. In comparisons between the ANI and HC groups, significant differences in the ECM values were found in four regions: ANI group patients showed increased ECM values in the left medial and paracingulate gyrus compared to the HC group, while the ECM values in the right superior parietal gyrus, left inferior parietal gyrus, and right middle frontal gyrus were significantly reduced. Additionally, when comparing the ANI and PWND groups, ANI patients exhibited decreased ECM values in the right inferior temporal gyrus, right insula, and right inferior frontal gyrus (GRF correction, voxel P=0.05, cluster P=0.05) (*Table 5*).

Correlation analysis results

The partial correlation analysis revealed significant associations between certain regional metrics and cognitive functions, as well as clinical information. In PWND patients, there was a negative correlation between ReHo in the right orbital middle frontal gyrus and information processing speed (r=–0.172, P=0.0272), and a negative correlation between ALFF in the right orbital superior frontal gyrus and abstract and executive function, cluster of differentiation (CD)4$^+$ T cell count, and CD4$^+$/CD8$^+$ ratio (r=–0.1768, P=0.0231; r=–0.2338, P=0.0074;

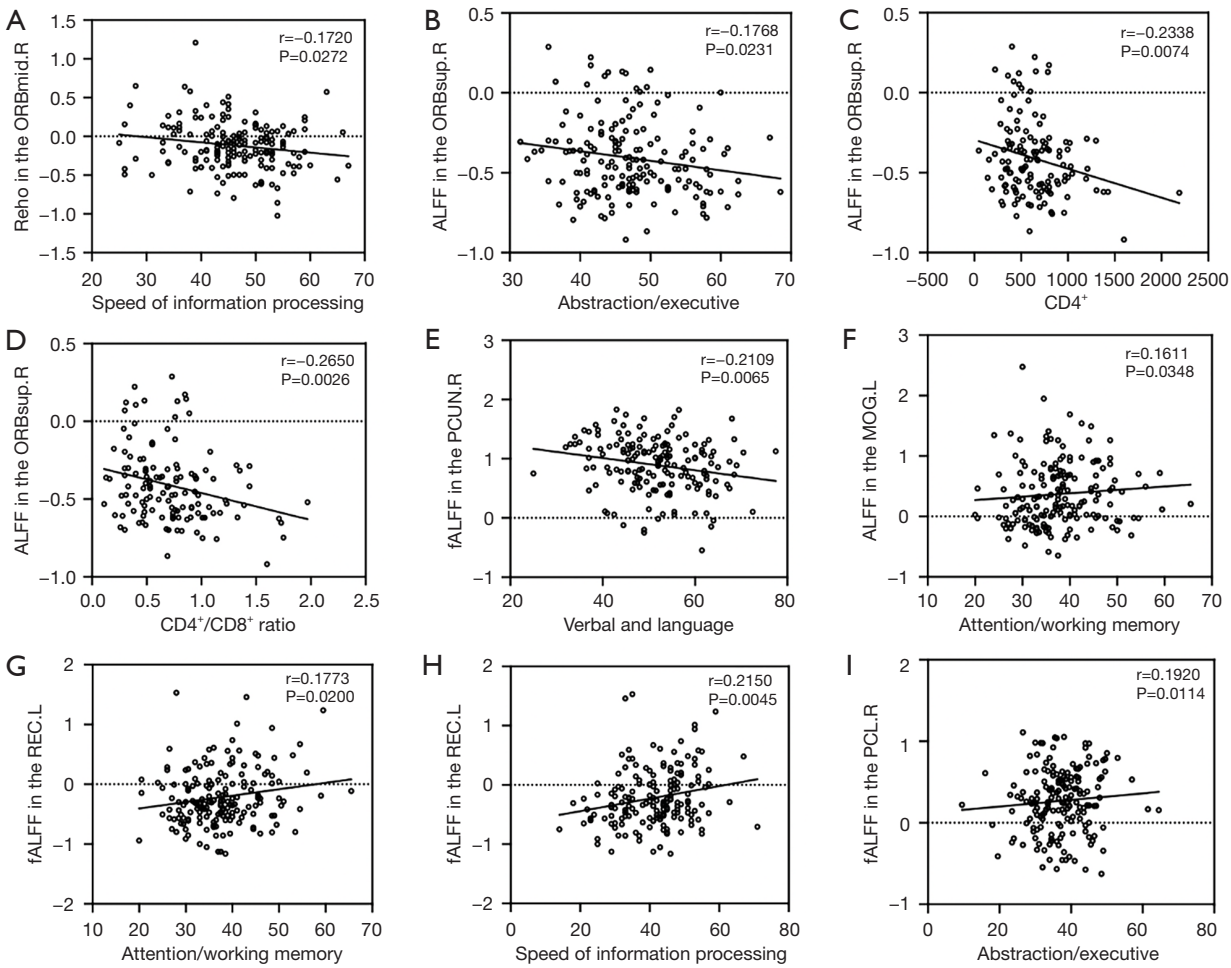

Figure 4 Correlation analysis results between rs-fMRI values, neuropsychological test results, and clinical laboratory indices in three groups. (A-E) Represent the PWND group, while (F-I) represent the ANI group. (A) ReHo in the right middle frontal gyrus showed a negative correlation with processing speed. (B) ALFF in the right orbital superior frontal gyrus showed a negative correlation with abstract and executive function. (C) ALFF in the right orbital superior frontal gyrus showed a negative correlation with $CD4^+$ count. (D) ALFF in the right orbital superior frontal gyrus showed a negative correlation with CD4/CD8 ratio. (E) fALFF in the right precuneus showed a negative correlation with verbal and language function. (F) ALFF in the left middle occipital gyrus showed a positive correlation with attention and working memory. (G) fALFF in the left straight gyrus showed a positive correlation with attention and working memory. (H) fALFF in the left straight gyrus showed a positive correlation with speed of information processing. (I) fALFF in the right paracentral lobule showed a positive correlation with abstract and executive function. ReHo, regional homogeneity; ALFF, amplitude of low-frequency fluctuation; fALFF, fractional amplitude of low-frequency fluctuation; ORBmid.R, right orbital frontal gyrus; ORBsup.R, right orbital superior frontal gyrus; PCUM.R, right anterior cuneiform lobe; MOG.L, left occipital gyrus; REC.L, left rectus gyri muscle; PCL.R, right paracentral lobule; rs-fMRI, resting-state functional magnetic resonance imaging; PWND, persons living with human immunodeficiency virus but without neurocognitive disorders; ANI, asymptomatic neurocognitive impairment.

r=−0.2650, P=0.0026). Further, a negative correlation was observed between fALFF in the right precuneus and verbal and language function (r=−0.2109, P=0.0065). In ANI patients, a positive correlation was found between ALFF in the left middle occipital gyrus and attention and working memory (r=0.1611, P=0.0348); between fALFF in the left straight gyrus and attention, working memory, and information processing speed (r=0.1773, P=0.0200; r=0.2150, P=0.0045); and between fALFF in the right paracentral lobule and abstract and executive function

Table 5 Regions showing significant differences in ECM between the groups

Variables	Contrast	Region	Network	MNI coordinates			*T* value	Cluster size
				X	Y	Z		
ECM	PWND > HCs	Cingulum_Mid_L	VAN	–12	–51	33	2.05258	619
	PWND < HCs	Precentral_R	SMN	66	6	18	–2.42305	2,140
	ANI > HCs	Cingulum_Mid_L	VAN	–12	–51	33	2.16719	444
	ANI < HCs	Parietal_Sup_R	DAN	24	–81	48	–2.00034	430
		Parietal_Inf_L	FPN	–48	–48	36	–2.25938	412
		Frontal_Mid_R	FPN	42	21	33	–2.45869	196
	ANI < PWND	Temporal_Inf_R	DAN	45	–9	–45	–2.80807	395
		Frontal_Inf_Oper_R	FPN	48	12	0	–2.34902	374
		Temporal_Inf_R	DAN	45	–51	–24	–2.80807	194

Coordinates (X, Y, Z) refer to the peak MNI coordinates of brain regions with peak intensity. A positive *t* value represents increased rs-fMRI values, while a negative *t* value represents decreased rs-fMRI values. The significance threshold was set at P<0.05. ECM, eigenvector centrality mapping; MNI, Montreal Neurological Institute; PWND, persons living with human immunodeficiency virus but without neurocognitive disorders; ANI, asymptomatic neurocognitive impairment; HCs, healthy controls; L, left; R, right; VAN, ventral attention network; SMN, somatomotor network; DAN, dorsal attention network; FPN, frontoparietal network.

(r=0.1920, P=0.0114) (*Figure 4*).

Discussion

Our study integrated regional and global metrics from rs-fMRI to undertake a comprehensive examination of local activity changes and global FC in PWND and ANI patients. We found that despite undetectable or very low levels of plasma HIV RNA, the HIV patients showed alterations in spontaneous brain activity irrespective of cognitive impairment, and these abnormalities were related to their clinical information and neurocognitive abilities. Specifically, we found that as their cognitive function declined, ReHo changes were mainly observed in the DMN, while ALFF decreases were observed in the parietal-occipital DMN and VIS, and increases were predominantly observed in the frontal and prefrontal regions, particularly in the limbic network (LIM). Both increases and decreases in fALFF were observed in the temporoparietal and subcortical regions, mainly involving decreases in the somatomotor network (SMN) and LIM, and increases in the DMN and LIM.

In contrast to the regional metrics, global FC was significantly reduced in both the PWND and ANI patients compared to the HCs. In the ANI group compared to the PWND group, some functional connections showed increases. The main brain networks affected by HIV infection included the DMN, SMN, and LIM. In comparison to the HCs, the DMN was the primary network affected in the ANI patients, while in comparison to the PWND patients, the ANI patients showed significant changes in the VIS, DMN, and LIM. These findings provide new theoretical insights that may lead to the identification of precise and comprehensive fMRI neuroimaging biomarkers for early brain cognitive assessment in PLWH.

Overall, we found that both global and local metrics tended to show consistent alterations across a wide range of changes, with the DMN, VIS, and LIM being the most extensively affected. The DMN, which plays a role in self-referential thinking, cognition, and emotional processing, is more active during rest than when an individual is performing tasks (33). Alterations in the DMN have been observed in many other neurological and psychiatric disorders (34). Previous studies have reported that HAND can lead to changes in FC within the DMN, and between the DMN and other networks (35,36). Further, DMN connectivity may serve as a potential biomarker for the early detection of simian immunodeficiency virus infection and for assessing the efficacy of related antiretroviral treatments (37). Visual network (VIS) abnormalities have also been noted in previous studies. Han *et al.* discovered that the VIS may be the brain region most affected by HIV infection in young individuals with ANI (38). Ances

et al. observed significantly reduced regional cerebral blood flow in the visual cortex of individuals with HIV infection using perfusion imaging (19). We hypothesize that these changes may be closely related to neuronal loss in the calcarine area of the primary visual cortex (39). Our findings support and extend previous functional neuroimaging studies in HIV populations, including those that have reported extensive functional alterations in the LIM. This is consistent with the findings of Zhou *et al.*, who reported widespread cortical atrophy and FC abnormalities involving regions such as the thalamus and hippocampus (40). These changes are likely associated with the regulation of emotions, sleep, circadian rhythms, temperature, and body weight.

Additionally, some of the brain regions showing significant changes in local metrics in this study also overlap with those identified in previous research. Bak *et al.* (41) found alterations in local intrinsic activity in the frontal lobe of HIV patients, irrespective of their cognitive status. These functional changes were highly correlated with reduced verbal memory and executive function in HIV patients. Using positron emission tomography, Vera *et al.* (42) observed increased translocator protein expression in the parieto-occipital region, indicating neuroinflammation. Additionally, Babiloni *et al.* (43) discovered significantly reduced resting-state electroencephalogram rhythms in the temporo-parieto-occipital regions of HIV patients. In terms of global metrics, the most notable reduction in FC in the PWND group compared to the HC group was observed between the right insula and the right supramarginal gyrus (between the VAN). This diminished FC might lead to deficits in "bottom-up" attention (effective attention shifting) (44), potentially due to reduced tonic activity of the locus coeruleus-norepinephrine system (45). We hypothesize that this could be associated with dopaminergic dysfunction following HIV infection (46).

Compared to the HC group, the most significant reduction in FC was between the right caudate nucleus (part of the salience network) and the left middle frontal gyrus (part of the FPN) in the ANI group. Multiple studies have found that HIV infection is associated with damage to the fronto-striatal pathway (47-49). This system comprises neural circuits connecting the cortex and basal ganglia. When HIV-1 enters the central nervous system, the HIV-1 viral proteins Tat and gp120 target regions rich in dopamine within the cortico-striatal circuits, leading to dopaminergic system dysfunction (50).

In our study, the PWND group exhibited patterns of intrinsic brain activation and connectivity changes similar to those observed in the ANI group. This suggests that even in the absence of clinical symptoms or neuropsychological abnormalities, the brain function of HIV patients is affected by the release of viral proteins (Tat and gp120), glutamate accumulation, dopaminergic dysregulation, pro-inflammatory factors [e.g., tumor necrosis factor-alpha (TNFα), interleukin-6 (IL-6), and interleukin-1 alpha (IL-1α)], and oxidative stress [e.g., nitric oxide (NO)], leading to neuronal damage and apoptosis (46). fMRI is highly sensitive in detecting the early neurobiological effects of the virus, and can measure such changes to a certain extent, and thus could potentially identify early changes in HIV-infected individuals without overt cognitive impairment. Therefore, more extensive cognitive testing needs to be performed in future research to reveal earlier changes in cognitive function. Additionally, the more extensive changes observed in the ANI versus HC comparison compared to the PWND versus HC comparison indicate that brain function continues to alter as the disease progresses. The seemingly paradoxical results of increased and decreased activity in the same network across different measures, as well as simultaneous increases and decreases in the functionality of different networks, may reflect compensatory regulation in abnormal brain regions. Reduced efficiency in certain brain areas may be offset by activation in other regions, a compensatory mechanism previously reported in studies of HIV patients (51).

The graph theory results corroborated the local metrics findings from different methodological perspectives. First, changes reflected in NE and NLE were notably concentrated in the DMN, indicating the stability of regional changes and further underscoring the significance of the DMN. Second, similar to local metrics, graph theory metrics showed corresponding increases and decreases; however, the primary alterations in ECM were observed in the FPN and dorsal attention network (DAN), which differs from our findings. It is worth noting that similar network changes have been mentioned previously (52,53). Additionally, previous studies have identified discrepancies in ECM results compared to other metrics; however, these discrepancies are likely due to methodological differences (54), as ECM is estimated based on an adjacency matrix that contains pairwise correlations between ROIs. A multifaceted methodological approach should be employed for the comprehensive monitoring of HAND.

Further, the correlation analysis revealed that increased ALFF in the right orbitofrontal superior gyrus

was negatively correlated with abstract and executive function performance, $CD4^+$ count, and the $CD4^+/CD8^+$ ratio. Similarly, increased fALFF in the right precuneus showed an inverse relationship with verbal and language performance. This implies that the degree of compensatory activation may increase as patients' neurocognitive and immune functions decline, which is consistent with findings from primate studies (55). Although changes in several local and global metrics were associated with neurocognitive scores, the neuroimaging results did not entirely align with the cognitive functions of the specific brain regions. Instead, they exhibited a complexity that spanned across brain networks. We propose several reasons for this phenomenon. First, cognitive functions are complex and high-level processes that typically involve the participation of multiple networks. The execution of a single cognitive function may engage multiple circuits and be regulated by various brain regions (56). Second, when cognitive impairment occurs due to disease-induced disruptions in brain homeostasis, brain regions exhibit high plasticity and can undergo reorganization to achieve functional compensation. Finally, the cognitive domains assessed in our study did not fully cover the entire spectrum of complex brain functions, which introduced a certain bias. However, we also observed that the correlations between imaging metrics and clinical information were negative in the PWND group, but were entirely positive in the ANI group. This discrepancy may reflect the lagging nature of clinical indicators, suggesting that neuroimaging can provide us with more sensitive biological markers.

Limitations

This study had some limitations. First, it focused exclusively on young and middle-aged male patients, which might limit the applicability of the findings to the general population or to female patients. Second, the study was conducted at a single-center with a relatively small sample size, and the diagnosis of ANI might have been influenced by individual short-term variations, which might have led to selection bias. Additionally, the neuroimaging results lack validation from pathological findings and basic experiments, and thus need to be confirmed in larger-scale studies. Third, as a cross-sectional study, it is subject to inherent biases and does not allow for the tracking of changes in brain function over the course of disease progression. A longitudinal study could more powerfully and objectively reveal these changes.

Data sharing policies and future directions

To promote transparency and foster collaboration in the study of brain function changes in HIV patients, we are committed to sharing the resources generated in this study. The de-identified rs-fMRI data of 438 HIV patients, along with the relevant metadata, will be made available on a publicly accessible platform such as OpenNeuro, pending approval from the relevant ethics committees. Researchers will be able to request access to the dataset for academic purposes through a formal application process, ensuring compliance with institutional guidelines and patient privacy protections. Access to the coding data will also be available upon reasonable request to the corresponding author.

Looking ahead, we aim to expand this work by collaborating with international cohorts, enabling cross-cultural comparisons and a deeper understanding of the global impact of HIV on brain function. We plan to explore the integration of larger, multi-site datasets, leveraging advanced analytical techniques to further elucidate region-specific and universal patterns of brain function alterations in HIV patients. These future endeavors will not only strengthen the current findings but also provide valuable insights into the broader neurological effects of HIV across diverse populations.

Conclusions

Through the analysis of local metrics (ReHo, ALFF, and fALFF), global metrics (FC), and graph theory metrics, we confirmed that HIV patients exhibit complex changes in both local brain activity and FC between brain regions, regardless of cognitive impairment. Some of these changes are linked to clinical information and neurocognitive abilities. Our findings indicate that the DMN, VIS, and LIM may be the areas in which early brain functional changes are most pronounced in HIV patients. The weakened connectivity within the VAN in PWND warrants further investigation, and damage to the fronto-striatal pathway may also play a significant role in the decline of cognitive function in individuals with HAND. Moreover, a multifaceted methodological approach should be employed for the comprehensive monitoring of HAND. Given that PLWH face lifelong brain damage due to HIV, which continuously affects cognitive function, there is an urgent need for accurate HAND biomarkers to aid in precise diagnosis, innovative treatment strategies, and long-term disease monitoring. This study provides new neuroimaging

evidence for early cognitive impairment in PLWH.

Acknowledgments

Funding: This work was supported by funding from the Beijing Hospital Authority Clinical Medicine Development Special Funding Support (No. ZLRK202333), the National Natural Science Foundation of China (Nos. 61936013 and 82271963), the Beijing Municipal Natural Science Foundation (Nos. 7212051 and L222097), and the Open Project of Henan Clinical Research Center of Infectious Diseases (AIDS) (No. KFKT202403).

Footnote

Reporting Checklist: The authors have completed the STROBE reporting checklist. Available at https://qims.amegroups.com/article/view/10.21037/qims-24-1342/rc

Conflicts of Interest: All authors have completed the ICMJE uniform disclosure form (available at https://qims.amegroups.com/article/view/10.21037/qims-24-1342/coif). The authors have no conflicts of interest to declare.

Ethical Statement: The authors are accountable for all aspects of the work in ensuring that questions related to the accuracy or integrity of any part of the work are appropriately investigated and resolved. This study was conducted in accordance with the Declaration of Helsinki (as revised in 2013) and was approved by the Medical Ethics Committee of Beijing Youan Hospital (No. LL-2020-047-K). Written informed consent was obtained from all participants.

References

1. Farhadian S, Patel P, Spudich S. Neurological Complications of HIV Infection. Curr Infect Dis Rep 2017;19:50.
2. Vastag Z, Fira-Mladinescu O, Rosca EC. HIV-Associated Neurocognitive Disorder (HAND): Obstacles to Early Neuropsychological Diagnosis. Int J Gen Med 2022;15:4079-90.
3. Antinori A, Arendt G, Becker JT, Brew BJ, Byrd DA, Cherner M, et al. Updated research nosology for HIV-associated neurocognitive disorders. Neurology 2007;69:1789-99.
4. Heaton RK, Clifford DB, Franklin DR Jr, Woods SP, Ake C, Vaida F, et al. HIV-associated neurocognitive disorders persist in the era of potent antiretroviral therapy: CHARTER Study. Neurology 2010;75:2087-96.
5. Biswal B, Yetkin FZ, Haughton VM, Hyde JS. Functional connectivity in the motor cortex of resting human brain using echo-planar MRI. Magn Reson Med 1995;34:537-41.
6. Viviano JD, Buchanan RW, Calarco N, Gold JM, Foussias G, Bhagwat N, Stefanik L, Hawco C, DeRosse P, Argyelan M, Turner J, Chavez S, Kochunov P, Kingsley P, Zhou X, Malhotra AK, Voineskos AN; Social Processes Initiative in Neurobiology of the Schizophrenia(s) Group. Resting-State Connectivity Biomarkers of Cognitive Performance and Social Function in Individuals With Schizophrenia Spectrum Disorder and Healthy Control Subjects. Biol Psychiatry 2018;84:665-74.
7. van den Heuvel MP, Hulshoff Pol HE. Exploring the brain network: a review on resting-state fMRI functional connectivity. Eur Neuropsychopharmacol 2010;20:519-34.
8. Tononi G, Sporns O, Edelman GM. A measure for brain complexity: relating functional segregation and integration in the nervous system. Proc Natl Acad Sci U S A 1994;91:5033-7.
9. Jiang L, Zuo XN. Regional Homogeneity: A Multimodal, Multiscale Neuroimaging Marker of the Human Connectome. Neuroscientist 2016;22:486-505.
10. Zang YF, He Y, Zhu CZ, Cao QJ, Sui MQ, Liang M, Tian LX, Jiang TZ, Wang YF. Altered baseline brain activity in children with ADHD revealed by resting-state functional MRI. Brain Dev 2007;29:83-91.
11. Zou QH, Zhu CZ, Yang Y, Zuo XN, Long XY, Cao QJ, Wang YF, Zang YF. An improved approach to detection of amplitude of low-frequency fluctuation (ALFF) for resting-state fMRI: fractional ALFF. J Neurosci Methods 2008;172:137-41.
12. Zhao J, Chen F, Ren M, Li L, Li A, Jing B, Li H. Low-

frequency fluctuation characteristics in rhesus macaques with SIV infection: a resting-state fMRI study. J Neurovirol 2019;25:141-9.
13. Li R, Wang W, Wang Y, Peters S, Zhang X, Li H. Effects of early HIV infection and combination antiretroviral therapy on intrinsic brain activity: a cross-sectional resting-state fMRI study. Neuropsychiatr Dis Treat 2019;15:883-94.
14. Yadav SK, Gupta RK, Hashem S, Bhat AA, Garg RK, Venkatesh V, Gupta PK, Singh AK, Chaturvedi S, Ahmed SN, Azeem MW, Haris M. Changes in resting-state functional brain activity are associated with waning cognitive functions in HIV-infected children. Neuroimage Clin 2018;20:1204-10.
15. Wang P, Li J, Wang X, Thapa D, Wu GY. Asymptomatic Human Immunodeficiency Virus Vertical Transmitted Adolescents' Brain Functional Changes: Based on Resting-State Functional Magnetic Resonance Imaging. AIDS Res Hum Retroviruses 2018;34:699-704.
16. Lee WH, Frangou S. Linking functional connectivity and dynamic properties of resting-state networks. Sci Rep 2017;7:16610.
17. Janssen MAM, Hinne M, Janssen RJ, van Gerven MA, Steens SC, Góraj B, Koopmans PP, Kessels RPC. Resting-state subcortical functional connectivity in HIV-infected patients on long-term cART. Brain Imaging Behav 2017;11:1555-60.
18. Wang H, Li R, Zhou Y, Wang Y, Cui J, Nguchu BA, Qiu B, Wang X, Li H. Altered cerebro-cerebellum resting-state functional connectivity in HIV-infected male patients. J Neurovirol 2018;24:587-96.
19. Ances BM, Sisti D, Vaida F, Liang CL, Leontiev O, Perthen JE, Buxton RB, Benson D, Smith DM, Little SJ, Richman DD, Moore DJ, Ellis RJ; HNRC group. Resting cerebral blood flow: a potential biomarker of the effects of HIV in the brain. Neurology 2009;73:702-8.
20. Ances BM, Vaida F, Yeh MJ, Liang CL, Buxton RB, Letendre S, McCutchan JA, Ellis RJ. HIV infection and aging independently affect brain function as measured by functional magnetic resonance imaging. J Infect Dis 2010;201:336-40.
21. Invernizzi A, Rechtman E, Oluyemi K, Renzetti S, Curtin P, Colicino E, Ambrosi C, Mascaro L, Patrono A, Corbo D, Cagna G, Gasparotti R, Reichenberg A, Tang CY, Smith DR, Placidi D, Lucchini RG, Wright RO, Horton MK. Topological network properties of resting-state functional connectivity patterns are associated with metal mixture exposure in adolescents. Front Neurosci 2023;17:1098441.
22. Invernizzi A, Rechtman E, Curtin P, Papazaharias DM, Jalees M, Pellecchia AC, Santiago-Michels S, Bromet EJ, Lucchini RG, Luft BJ, Clouston SA, Tang CY, Horton MK. Functional changes in neural mechanisms underlying post-traumatic stress disorder in World Trade Center responders. Transl Psychiatry 2023;13:239.
23. Aili X, Wang W, Zhang A, Jiao Z, Li X, Rao B, Li R, Li H. Rich-Club Analysis of Structural Brain Network Alterations in HIV Positive Patients With Fully Suppressed Plasma Viral Loads. Front Neurol 2022;13:825177.
24. Yagi S, Lee A, Truter N, Galea LAM. Sex differences in contextual pattern separation, neurogenesis, and functional connectivity within the limbic system. Biol Sex Differ 2022;13:42.
25. Chang L, Løhaugen GC, Douet V, Miller EN, Skranes J, Ernst T. Neural correlates of working memory training in HIV patients: study protocol for a randomized controlled trial. Trials 2016;17:62.
26. Gandhi NS, Skolasky RL, Peters KB, Moxley RT 4th, Creighton J, Roosa HV, Selnes OA, McArthur J, Sacktor N. A comparison of performance-based measures of function in HIV-associated neurocognitive disorders. J Neurovirol 2011;17:159-65.
27. Shi C, Kang L, Yao S, Ma Y, Li T, Liang Y, Cheng Z, Xu Y, Shi J, Xu X, Zhang C, Franklin DR, Heaton RK, Jin H, Yu X. The MATRICS Consensus Cognitive Battery (MCCB): Co-norming and standardization in China. Schizophr Res 2015;169:109-15.
28. Zang Y, Jiang T, Lu Y, He Y, Tian L. Regional homogeneity approach to fMRI data analysis. Neuroimage 2004;22:394-400.
29. Friston KJ, Williams S, Howard R, Frackowiak RS, Turner R. Movement-related effects in fMRI time-series. Magn Reson Med 1996;35:346-55.
30. Wink AM, de Munck JC, van der Werf YD, van den Heuvel OA, Barkhof F. Fast eigenvector centrality mapping of voxel-wise connectivity in functional magnetic resonance imaging: implementation, validation, and interpretation. Brain Connect 2012;2:265-74.
31. Demaria G, Invernizzi A, Ombelet D, Carvalho JC, Renken RJ, Cornelissen FW. Binocular Integrated Visual Field Deficits Are Associated With Changes in Local Network Function in Primary Open-Angle Glaucoma: A Resting-State fMRI Study. Front Aging Neurosci 2021;13:744139.
32. Invernizzi A, Halbertsma HN, van Ackooij M, Bais

L, Boertien J, Renken RJ, Cornelissen FW, van Laar T. rTMS treatment of visual hallucinations using a connectivity-based targeting method - A case study. Brain Stimul 2019;12:1622-4.
33. Smitha KA, Akhil Raja K, Arun KM, Rajesh PG, Thomas B, Kapilamoorthy TR, Kesavadas C. Resting state fMRI: A review on methods in resting state connectivity analysis and resting state networks. Neuroradiol J 2017;30:305-17.
34. Gonen OM, Kwan P, O'Brien TJ, Lui E, Desmond PM. Resting-state functional MRI of the default mode network in epilepsy. Epilepsy Behav 2020;111:107308.
35. Thomas JB, Brier MR, Snyder AZ, Vaida FF, Ances BM. Pathways to neurodegeneration: effects of HIV and aging on resting-state functional connectivity. Neurology 2013;80:1186-93.
36. Thomas J, Sharma D, Mohanta S, Jain N. Resting-State functional networks of different topographic representations in the somatosensory cortex of macaque monkeys and humans. Neuroimage 2021;228:117694.
37. Tang ZC, Liu JJ, Ding XT, Liu D, Qiao HW, Huang XJ, Zhang H, Tian J, Li HJ. The default mode network is affected in the early stage of simian immunodeficiency virus infection: a longitudinal study. Neural Regen Res 2023;18:1542-7.
38. Han S, Aili X, Ma J, Liu J, Wang W, Yang X, Wang X, Sun L, Li H. Altered regional homogeneity and functional connectivity of brain activity in young HIV-infected patients with asymptomatic neurocognitive impairment. Front Neurol 2022;13:982520.
39. Everall IP, Luthert PJ, Lantos PL. Neuronal number and volume alterations in the neocortex of HIV infected individuals. J Neurol Neurosurg Psychiatry 1993;56:481-6.
40. Zhou Y, Li R, Wang X, Miao H, Wei Y, Ali R, Qiu B, Li H. Motor-related brain abnormalities in HIV-infected patients: a multimodal MRI study. Neuroradiology 2017;59:1133-42.
41. Bak Y, Jun S, Choi JY, Lee Y, Lee SK, Han S, Shin NY. Altered intrinsic local activity and cognitive dysfunction in HIV patients: A resting-state fMRI study. PLoS One 2018;13:e0207146.
42. Vera JH, Guo Q, Cole JH, Boasso A, Greathead L, Kelleher P, Rabiner EA, Kalk N, Bishop C, Gunn RN, Matthews PM, Winston A. Neuroinflammation in treated HIV-positive individuals: A TSPO PET study. Neurology 2016;86:1425-32.
43. Babiloni C, Buffo P, Vecchio F, Onorati P, Muratori C, Ferracuti S, Roma P, Battuello M, Donato N, Noce G, Di Campli F, Gianserra L, Teti E, Aceti A, Soricelli A, Viscione M, Andreoni M, Rossini PM, Pennica A. Cortical sources of resting-state EEG rhythms in "experienced" HIV subjects under antiretroviral therapy. Clin Neurophysiol 2014;125:1792-802.
44. Vossel S, Geng JJ, Fink GR. Dorsal and ventral attention systems: distinct neural circuits but collaborative roles. Neuroscientist 2014;20:150-9.
45. Corbetta M, Patel G, Shulman GL. The reorienting system of the human brain: from environment to theory of mind. Neuron 2008;58:306-24.
46. González-Scarano F, Martín-García J. The neuropathogenesis of AIDS. Nat Rev Immunol 2005;5:69-81.
47. Ortega M, Brier MR, Ances BM. Effects of HIV and combination antiretroviral therapy on cortico-striatal functional connectivity. AIDS 2015;29:703-12.
48. Plessis SD, Vink M, Joska JA, Koutsilieri E, Stein DJ, Emsley R. HIV infection and the fronto-striatal system: a systematic review and meta-analysis of fMRI studies. AIDS 2014;28:803-11.
49. Plessis Sd, Vink M, Joska JA, Koutsilieri E, Bagadia A, Stein DJ, Emsley R. HIV infection results in ventral-striatal reward system hypo-activation during cue processing. AIDS 2015;29:1335-43.
50. Gaskill PJ, Miller DR, Gamble-George J, Yano H, Khoshbouei H. HIV, Tat and dopamine transmission. Neurobiol Dis 2017;105:51-73.
51. Melrose RJ, Tinaz S, Castelo JM, Courtney MG, Stern CE. Compromised fronto-striatal functioning in HIV: an fMRI investigation of semantic event sequencing. Behav Brain Res 2008;188:337-47.
52. Luckett PH, Paul RH, Hannon K, Lee JJ, Shimony JS, Meeker KL, Cooley SA, Boerwinkle AH, Ances BM. Modeling the Effects of HIV and Aging on Resting-State Networks Using Machine Learning. J Acquir Immune Defic Syndr 2021;88:414-9.
53. Egbert AR, Biswal B, Karunakaran KD, Pluta A, Wolak T, Rao S, Bornstein R, Szymańska B, Horban A, Firląg-Burkacka E, Sobańska M, Gawron N, Bieńkowski P, Sienkiewicz-Jarosz H, Ścińska-Bieńkowska A, Łojek E. HIV infection across aging: Synergistic effects on intrinsic functional connectivity of the brain. Prog Neuropsychopharmacol Biol Psychiatry 2019;88:19-30.
54. Chang L, Tomasi D, Yakupov R, Lozar C, Arnold S, Caparelli E, Ernst T. Adaptation of the attention network in human immunodeficiency virus brain injury. Ann Neurol 2004;56:259-72.

55. Zhao J, Jing B, Chen F, Liu J, Wang Y, Li H. Altered regional homogeneity of brain spontaneous signals in SIV infected rhesus macaque model. Magn Reson Imaging 2017;37:56-61.

56. Damoiseaux JS, Rombouts SA, Barkhof F, Scheltens P, Stam CJ, Smith SM, Beckmann CF. Consistent resting-state networks across healthy subjects. Proc Natl Acad Sci U S A 2006;103:13848-53.

Cite this article as: Jiang X, Hou C, Ma J, Li H. Alterations in local activity and whole-brain functional connectivity in human immunodeficiency virus-associated neurocognitive disorders: a resting-state functional magnetic resonance imaging study. Quant Imaging Med Surg 2025;15(1):563-580. doi: 10.21037/qims-24-1342